Remote Sensing of Environment 221 (2019) 38–49

Contents lists available at ScienceDirect

Remote Sensing of Environment

journal homepage: www.elsevier.com/locate/rse

Detecting prairie biodiversity with airborne remote sensing

Hamed Gholizadeh[a,*], John A. Gamon[a,b,c], Philip A. Townsend[d], Arthur I. Zygielbaum[a], Christopher J. Helzer[e], Gabriel Y. Hmimina[a], Rong Yu[a], Ryan M. Moore[a], Anna K. Schweiger[f], Jeannine Cavender-Bares[f]

[a] Center for Advanced Land Management Information Technologies, School of Natural Resources, University of Nebraska-Lincoln, Lincoln, NE 68583, USA
[b] Department of Earth and Atmospheric Sciences, University of Alberta, Edmonton, AB T6G 2E3, Canada
[c] Department of Biological Sciences, University of Alberta, Edmonton, AB T6G 2R3, Canada
[d] Department of Forest and Wildlife Ecology, University of Wisconsin-Madison, Madison, WI 53706, USA
[e] Nebraska Director of Science, The Nature Conservancy, Aurora, NE 68818, USA
[f] Department of Ecology, Evolution and Behavior, University of Minnesota, Saint Paul, MN 55108, USA

ARTICLE INFO

Keywords:
Biodiversity
Airborne remote sensing
Spectral diversity
α-Diversity
Restored prairie
Spatial scale
Invasion

ABSTRACT

This study assessed the application of airborne imaging spectroscopy to monitor α-diversity in restored grassland plots. The study site was located within the Central Platte River ecosystem, south of Wood River in Central Nebraska, USA, and consisted of two sets of plots (young and old). Exotic species had recently invaded the old plots, confounding the original study design, while the young plots did not have significant invasion by weeds, reflecting the original study design. We used spectral variation (i.e. spectral diversity, expressed as the coefficient of variation) as a proxy for α-diversity (expressed as species richness and Shannon index). Airborne data collected at two flight altitudes and two flight directions tested the validity of "spectral diversity-α-diversity" relationship at different sampling scales and flight directions. Our results showed a strong relationship between spectral diversity and α-diversity in young, non-invaded plots exhibiting strong differences in α-diversity. However, in the old, invaded plots, the spectral diversity-α-diversity relationship was non-significant. Factors likely contributing to this failure in the old plots included the spatial mismatch between airborne and field-based sampling, the convergence in diversity levels over time, and the unique reflectance signatures of the invasive species related to their different structural and phenological properties. Unlike previous airborne studies in manipulated experimental prairie plots, but similar to results in more natural settings, the strong spectral diversity-α-diversity relationship in the young plots remained even at the spatial resolution of 1 m, demonstrating the potential of airborne remote sensing to assess diversity patterns in prairie grasslands. These findings demonstrate the importance of experimental remote sensing in evaluating spectral diversity, and provide insight for the development of operational airborne methods to assess biodiversity.

1. Introduction

Grasslands provide services vital for human well-being such as biomass production, water storage, belowground carbon storage, and nutrient cycling (Naeem et al., 2016; Wall et al., 2015). Unfortunately, grasslands are threatened by climate change, overgrazing, and conversion to agricultural use (Clark and Tilman, 2008; Oldeman, 1994; Ramankutty et al., 2008). Loss of grasslands has resulted in the loss of biodiversity with negative impacts on ecosystem function and ecosystem resistance to disturbances (Bevans, 2017; Chapin et al., 1998; Hooper et al., 2012; Tilman et al., 2012; Villnäs et al., 2013). Native grasslands, often called prairie in North America, once covered about 38% of United States land surface (Weaver, 1954). Since European settlement began, however, most native grasslands have been lost (Samson and Knopf, 1994). With the continuous destruction of grasslands and associated loss of biodiversity, ongoing monitoring and restoration of grasslands remains a high priority (Schramm, 1990; Suding, 2011).

Traditionally, biodiversity monitoring relies on field inventories that usually cover small geographical regions. While the information from such field campaigns is valuable, collecting species information over a large geographical extent is challenging. Consequently, there is a gap in our understanding of and ability to track changes in biodiversity at global scales, and remote sensing is often invoked as a way to fill this

* Corresponding author.
E-mail address: hamed.gholizadeh@unl.edu (H. Gholizadeh).

https://doi.org/10.1016/j.rse.2018.10.037
Received 8 June 2018; Received in revised form 25 October 2018; Accepted 30 October 2018
Available online 09 November 2018

gap (Cavender-Bares et al., 2017; Jetz et al., 2016). While remote sensing is not able to provide the same level of detailed biodiversity information as ground-based measurements, it may serve as a critical source of biodiversity information at larger scales than can be provided by traditional field methods, and offers the potential for continuous, consistent monitoring over time (Turner, 2014). Remotely sensed data coupled with and referenced to ground-based measurements may be the best (and most cost efficient) solution for global biodiversity monitoring (Buchanan et al., 2009; Gillespie et al., 2008; Kerr and Ostrovsky, 2003; Turner et al., 2003).

Remote sensing (here focusing on passive optical remote sensing) has been used to map species distribution and study the linkage between spectral data and biodiversity (Nagendra, 2001; Rocchini et al., 2010) mainly by 1) detecting single species if high spatial resolution data are available, or 2) classifying the habitat and studying the association between biodiversity and land cover (Gougeon, 1995; Schäfer et al., 2016). These two approaches have been mainly applied to vegetation types with large canopies such as forests (Asner et al., 2008; Schäfer et al., 2016).

Unlike forests, relatively little work has been done to study biodiversity in grasslands using remote sensing. In grasslands, remotely sensed data have been mostly used for classifying grasslands and distinguishing them from other land cover types (Baldi et al., 2006; Tovar et al., 2013; Wang et al., 2010), estimating quantities such as their aboveground biomass and productivity (Seaquist et al., 2003), leaf area index (Darvishzadeh et al., 2011), and evapotranspiration (Kustas and Norman, 1996). The main challenge for remote sensing of biodiversity in grasslands is the small size of plants, which leads to difficulty in resolving individual species. Therefore, for mapping biodiversity in grasslands, a third approach known as spectral diversity (or optical diversity) has been proposed as a potential solution. The idea behind spectral diversity is that spectral variation is driven in part by biodiversity, expressed as variation in leaf traits, canopy structure, and phenology (Ustin and Gamon, 2010). This approach uses a subset or all spectral bands to map biodiversity (Carter et al., 2005; Dahlin, 2016; Oldeland et al., 2010; Ustin and Gamon, 2010). In this paper, instead of direct identification of species, we focus on spectral diversity as an abstract measure of biodiversity. Among the many dimensions of biodiversity (e.g. taxonomic, functional, phylogenetic, and genetic), this study concentrated on local taxonomic diversity (α-diversity), measured as species richness (i.e. the number of species in a community) and species evenness.

Spectral diversity can be applied to spectral data obtained from spaceborne, airborne, and proximal platforms. Several studies have used spaceborne remote sensing with coarse spatial resolutions for capturing species diversity in grasslands. However, the coarse spatial resolution of these spaceborne sensors means that each grain (i.e. pixel) contains many grassland plants, species, or even more than one vegetation type (Jetz et al., 2016; Rocchini et al., 2010; Turner, 2014). Therefore, such data represent the aggregate response from a large group of species and cannot easily capture α-diversity within communities. In grasslands, most biodiversity research using spaceborne data has focused on using spectral reflectance of individual bands or simple spectral transformations such as vegetation indices (Gaitán et al., 2013; Guo et al., 2015; Lauver, 1997), most of which can be considered as proxies of productivity or greenness. Although these quantities have shown to be linked with biodiversity in some cases, the mechanisms that link these quantities to biodiversity are not fully understood (Skidmore et al., 2015) and might be caused by factors linked to the productivity-biodiversity relationship, which itself is an ongoing topic of discussion (Waide et al., 1999). Currently, several spaceborne sensors are in the planning or design phase (Guanter et al., 2015; Lee et al., 2015); once these forthcoming hyperspectral sensors are launched and their data are available, the applicability of spaceborne data for biodiversity mapping in grasslands can be more fully investigated.

Given the limitations of current spaceborne data for biodiversity detection in grasslands, several studies have examined the application of spectral diversity in grasslands using airborne and proximal hyperspectral data (Gholizadeh et al., 2018; Schweiger et al., 2018; Wang et al., 2018; Wang et al., 2016). Although these studies all showed a positive relationship between spectral diversity and α-diversity, most were conducted at the Cedar Creek Ecosystem Science Reserve in Central Minnesota, USA, where the strength of the relationship between spectral diversity and α-diversity was shown to be influenced by confounding factors such as soil exposure and spatial resolution of remote sensing data with respect to plot size (Gholizadeh et al., 2018). Due to the particular design of biodiversity field experiments, many of which involve small plots (< 10 m size) maintained at specific species richness levels, transferring the knowledge gained from experimental systems to "real world" applications remains a challenge, particularly for grasslands.

To address this challenge in grasslands, as our first objective, we tested the capability of airborne remote sensing to characterize the spectral diversity-α-diversity relationship (considering both species richness and evenness) using the coefficient of variation (CV) in spectral reflectance. Our previous work at the Cedar Creek Ecosystem Science Reserve in Central Minnesota, USA showed that spatial scale is a crucial factor in remote sensing of biodiversity (Gholizadeh et al., 2018; Wang et al., 2018). As our second objective, we investigated the scale dependence of spectral diversity by flying our airborne sensor at two different altitudes and generating several additional data sets with coarser spatial resolutions through spatial resampling. Here, we limit our discussion of scale to its spatial (not spectral) aspect, and specifically its grain (or pixel) size rather than the extent of the study area. Finally, vegetation surfaces are non-Lambertian (non-isotropic), and therefore, reflectance spectra change in accord with sun-target-sensor geometry (Goodin et al., 2004; Ranson et al., 1985; Shibayama and Wiegand, 1985) and are affected by shadows and hotspot effects (Calleja et al., 2016; Camacho de Coca et al., 2001). Therefore, as our third objective, we explored the effect of sampling geometry and tested how flight direction affects the spectral diversity-α-diversity relationship. Because of their potential influence on the detection of biodiversity, these technical issues must be considered in any operational methods of routinely assessing biodiversity from airborne sensors.

We evaluated the capability of airborne remote sensing to capture the spectral diversity-α-diversity relationship in a long-term grassland restoration experiment conducted by The Nature Conservancy at Wood River, NE. Unlike our previous experiment at Cedar Creek, our current study site at Wood River consists of plots with larger dimensions, higher species richness levels, and less manipulation (e.g. the plots were not affected by regular weeding). Therefore, the current study site provides a more "realistic" test of airborne biodiversity detection over Midwestern prairie, providing a unique opportunity to develop operational methods for remote sensing of biodiversity in grassland ecosystems.

2. Methods

2.1. Study area

The study area, maintained by The Nature Conservancy, is a prairie restoration study, along the Platte River, 10 km south of Wood River, NE (N 40°44′41″, W 98°35′11″; Fig. 1a). Prior to conversion to prairie (starting in 2006), this site had been a farmland planted in a corn-soybean rotation (Nemec et al., 2013). The study area consists of two fields and 36 60 × 60 m plots (some plots are slightly smaller than 60 × 60 m). One set of 24 plots, was seeded in 2006 (Fig. 1a, right), and these plots are referred to as "old plots." These plots were planted at two diversity levels and two seeding rates: 1) high diversity plots with low seeding rate (H) with measured species richness of 41.17 ± 2.48 (mean ± standard deviation), 2) high diversity plots with high seeding rate (H2; species richness of these plots was not measured in this study),

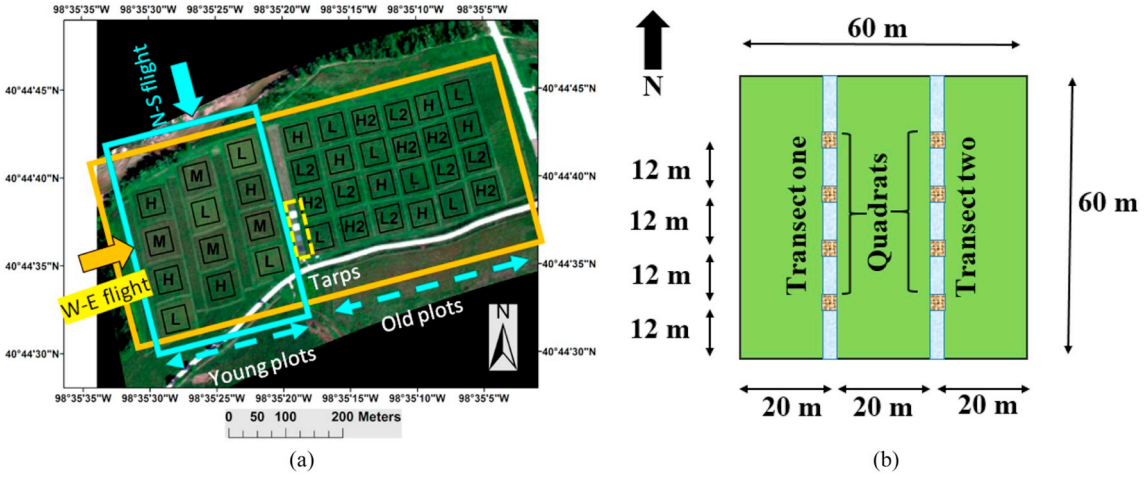

Fig. 1. (a) True color composite of the study area within the Central Platte River ecosystem, south of Wood River in Central Nebraska. H, M, and L indicate plots with high, medium, and low planted diversity, respectively. H2 and L2 indicate plots with high diversity/high seeding rate and low diversity/high seeding rate, respectively. We collected species data from the 24 plots shown by H, M, and L. Four calibration tarps can be seen in the yellow dashed box in the middle of the scene. The large orange box shows the area covered by the West-East flight, and the large cyan box shows the area covered by the North-South flight, and (b) diagram of a single plot showing the sampling design. (For interpretation of the references to color in this figure legend, the reader is referred to the web version of this article.)

Table 1
Data summary of the plots within the Central Platte River ecosystem, south of Wood River in Central Nebraska. Invasion level indicates cover of *Conium maculatum*, *Melilotus officinalis*, and *Bromus inermis* where none = 0% cover, low = 1–6% cover, medium = 7–15% cover, and high = 16–50% cover. For seeding rates at the Old plots see Nemec et al. (2013).

Experiment	Planted diversity level	Number of plots	Ground measurement	Invasion level		
				Conium maculatum	*Melilotus officinalis*	*Bromus inermis*
Young plots	High diversity ("H")	4	Yes	None	None to low	None
	Medium diversity ("M")	4	Yes	None	None	None
	Low diversity ("L")	4	Yes	None	None to high	None
Old plots	High diversity/low seeding rate ("H")	6	Yes	None to medium	Low to high	None to high
	Low diversity/low seeding rate ("L")	6	Yes	None to medium	Low to high	None to high
	High diversity/high seeding rate ("H2")	6	No	Not measured	Not measured	Not measured
	Low diversity/high seeding rate ("L2")	6	No	Not measured	Not measured	Not measured

3) low diversity plots with low seeding rate (L) with measured species richness of 37.83 ± 6.43, and 4) low diversity plots with high seeding rate (L2; species richness of these plots was not measured in this study). Another set of 12 plots (Fig. 1a, left) was seeded in 2010 at three diversity levels: low (L) with measured species richness of 16.75 ± 3.95, medium (M) with measured species richness of 32.50 ± 1.00, and high (H) with measured species richness of 44.25 ± 0.50. We refer to these plots as "young plots." Among these 36 plots, we chose 24 plots with comparable seeding rates (shown by letters H, M, and L in Fig. 1a) for analysis of the spectral diversity-α-diversity relationship. These include high, medium, and low diversity plots in the young plots as well as plots with high diversity/low seeding rate, and low diversity/low seeding rate in the old plots. A summary of plot treatments is presented in Table 1. Since conversion, the site has been managed with prescribed fires, and was last burned in late March 2015, two years prior to our study. A few noxious weeds (*Carduus nutans* in the old plots, *Hypericum perforatum* and *Lythrum salicaria* in the young plots) have been periodically removed via hand-pulling or spot-spraying as required by law, but there were no other manipulations of plant communities.

The species in this experiment consist of C_3 and C_4 grasses as well as forbs, and the most common species across all of the plots based on an August 2017 inventory include: *Andropogon gerardii*, *Poa pratensis**, *Panicum virgatum*, *Solidago gigantea*, and *Solidago canadensis* (asterisk indicates an exotic species based on the USDA Plants database, plants.usda.gov). Inventories were conducted by running two full length South-North transects (at 20 m and 40 m) through the plots, each 2 m wide (West-East). Within each transect, the presence or absence of each species was documented, and was considered present in the plot if it occurred within either transect. The percent cover of species used for evenness calculations was also documented by placing 0.5 m^2 (0.5 m by 1 m) quadrats at four points along each transect (at 12, 24, 36 and 48 m distance from the southern edge; eight quadrats per plot in total) and recording the percent cover in each of these to estimate an average value for the plot (see Fig. 1b for transect sampling design). The complete list of the species from the 2017 inventory can be found in Table A1 in Appendix 1.

Species composition of the plots within the old plots had significantly shifted since the start of the study by the spread of species between plots as shown by the number of planted species in the old plots vs. the number of observed species in Table A2 in Appendix 1 (the plot numbering scheme is shown in Fig. A1 in Appendix 1). In addition, the old plots were heavily affected by invasive species external to the study's seed mix, including poison hemlock (*Conium maculatum*), sweet clover (*Melilotus officinalis*), and smooth brome (*Bromus inermis*; which was intentionally added to the experiment in 2008) (Nemec et al., 2013). Bull thistle (*Cirsium vulgare*), a biennial plant, was also found previously to be invading the plots but was observed only infrequently in 2017. Percent cover of these three primary invasive species (*Conium maculatum*, *Melilotus officinalis*, and *Bromus inermis*) in each plot is presented in Table A3 in Appendix 1.

2.2. Airborne data collection and pre-processing

Airborne remote sensing data collection started at 10:14 AM local

Table 2
Flight details (August 23, 2017) over the biodiversity plots within the Central Platte River ecosystem, south of Wood River in Central Nebraska. Flight times are provided in local (Central) time, i.e. GMT – 5 h and represent daylight savings time.

Flight number	Flight direction	Local time	Spatial resolution (m)	Flight altitude above ground level (m)
Flight 1	North-South	10:14 AM	1	1396
Flight 2	West-East	10:20 AM		
Flight 3	North-South	10:28 AM	0.5	698
Flight 4	West-East	10:33 AM		

time (15:14 PM GMT) on August 23, 2017 using "CHAMP" (the CALMIT Hyperspectral Airborne Monitoring Platform), the University of Nebraska's aircraft operated by the UNL's Center for Advanced Land Management Information Technologies (CALMIT) equipped with a pushbroom hyperspectral sensor (AISA Kestrel, Specim, Oulu, Finland). This sensor covers 400–1000 nm with spectral resolution of 1.75 nm and field of view (FOV) of 40° under nadir viewing conditions. To increase the signal-to-noise ratio of the data, off-chip spectral binning (Dell'Endice, 2008) was applied. The final data set had 178 bands at approximately 3.5 nm intervals. We used bands between 427 and 914 nm (142 bands in total). To determine the impact of spatial scale on spectral diversity, we collected two data sets with spatial resolution (pixel sizes) of 0.5 m and 1 m by flying at two altitudes (698 m and 1396 m above ground level) in the near West-East direction (Table 2). To test the sensitivity of our results to flight direction and sampling geometry, we also repeated our flights over the young plots in the near North-South direction (due to the reduced swath width, covering both new and old plots in the North-South flight for the 0.5 m resolution image was not possible; Table 2). The West-East flight was almost parallel to the solar principal plane, and the direction of the North-South flight was orthogonal to that of the West-East flight. Ground control points collected in the field were used for georeferencing. Geometric distortions differed among flight lines, but because the plots in our experiment are large, with thousands of pixels within each plot, the effect of any mis-registration was considered minor.

Spectral reflectance signatures of four 10 × 10 m polyester calibration tarps (white, silver gray, charcoal, and black; Odyssey™, Marlen Textiles, New Haven, MO, USA) were measured using paired spectroradiometers (USB2000; Ocean Optics Inc., Dunedin, Florida, USA) during the overpass time of the airplane. One detector was equipped with a cosine corrector measuring downwelling irradiance to correct for minor atmospheric variation during the sampling period, and the other was equipped with a fiber optic (FOV of approximately 25°) measuring upwelling radiation. The spectral resolution of these sensors were ~1.5 nm covering ~350–1000 nm range. We also used a white reference panel (Spectralon, Labsphere, North Sutton, New Hampshire, USA) to calculate reflectance of the tarps. After removing outliers, reflectance data from each tarp were averaged and then resampled to match the wavelengths of the airborne sensor. The tarp reflectance data were then used to convert airborne radiance to reflectance using the empirical line correction method (Conel et al., 1987). To avoid edge effects, we defined equal-sized ~42 × 42 m regions inside all plots (young plots + old plots) and used these regions to calculate spectral diversity.

2.2.1. Generating coarse spatial resolution data from airborne data

To further investigate the impact of spatial scale on spectral diversity-α-diversity relationship, we used the 0.5 m resolution data from the West-East flight to generate data sets at coarser spatial resolutions (2, 3, 4, 5, and 6 m pixel sizes). This coarsened date set was simply generated by resampling and averaging the pixels of the 0.5 m resolution data. We refer to this data set as the "coarsened data set."

2.3. Spectral diversity metric

There are many methods that can be used to objectively calculate spectral diversity. Previous studies have shown that the performance of these spectral diversity metrics can vary significantly depending on factors such as spatial resolution, and there is no universally best metric (Gholizadeh et al., 2018). We tested several metrics (results are not shown here) including the coefficient of variation (CV), spectral angle mapper (Kruse et al., 1993), standard deviation of normalized difference vegetation index (NDVI), convex hull volume (Dahlin, 2016), convex hull area (Gholizadeh et al., 2018), and principal component analysis (Oldeland et al., 2010). Among these metrics, CV and standard deviation of NDVI showed the best performance, SAM was the second best metric, and the remaining metrics showed poor or non-significant relationships with field sampled α-diversity. We limited our analysis to CV as our primary spectral diversity metric for airborne data and used SAM to visualize spatial variability within the plots.

2.3.1. Plot-based analysis of spectral diversity-α-diversity

Using all pixels within a plot, we calculated CV for each band, and then used the CV averaged across bands as the spectral diversity of that plot. With this method, the spectral diversity of each plot is represented with a single CV value. The values of spectral diversity obtained from all pixels within plots were compared to species richness and Shannon index (Shannon, 1948) obtained from transect-based field sampling (Shannon index $= -\sum_{i=1}^{n} \alpha_i \ln(\alpha_i)$ where α is the abundance of the i^{th} species within a plot, n is the number of species, and "ln" is the natural logarithm).

2.3.2. Transect-based analysis of spectral diversity-α-diversity

To examine whether our species inventories (collected along transects in the field) match the plot-based spectral diversity (i.e. CV calculated using all pixels within plots in the airborne imagery) or transects-based spectral diversity (i.e. CV calculated using pixels within transects in the airborne imagery), we also ran a transect-based analysis of the spectral diversity-α-diversity relationship by using the pixels within each transect. For this analysis, we delineated the approximate locations of the transects (2-meter wide transects in each plot; Fig. 1b) in the airborne imagery and recalculated the spectral diversity-α-diversity relationship based on the pixels within the transects. Due to the mismatch between the field quadrat size and the scale of our remote sensing data (i.e. small size of these quadrats with respect to pixel size), a quadrat-based analysis of spectral diversity-α-diversity relationship was not feasible.

2.4. Mapping spatial variability within plots

Although CV was used as the spectral diversity metric in this study, it represents each plot with one number; therefore, it cannot show the within plot variation. To visualize the within-plot variability, we used spectral angle mapper (SAM; Kruse et al., 1993). SAM calculates the angle between two vectors:

$$\mathrm{SAM} = \arccos\left(\frac{R_{K,L}\cdot\overline{R}_L}{\|R_{K,L}\|_2\,\|\overline{R}_L\|_2}\right) \quad (1)$$

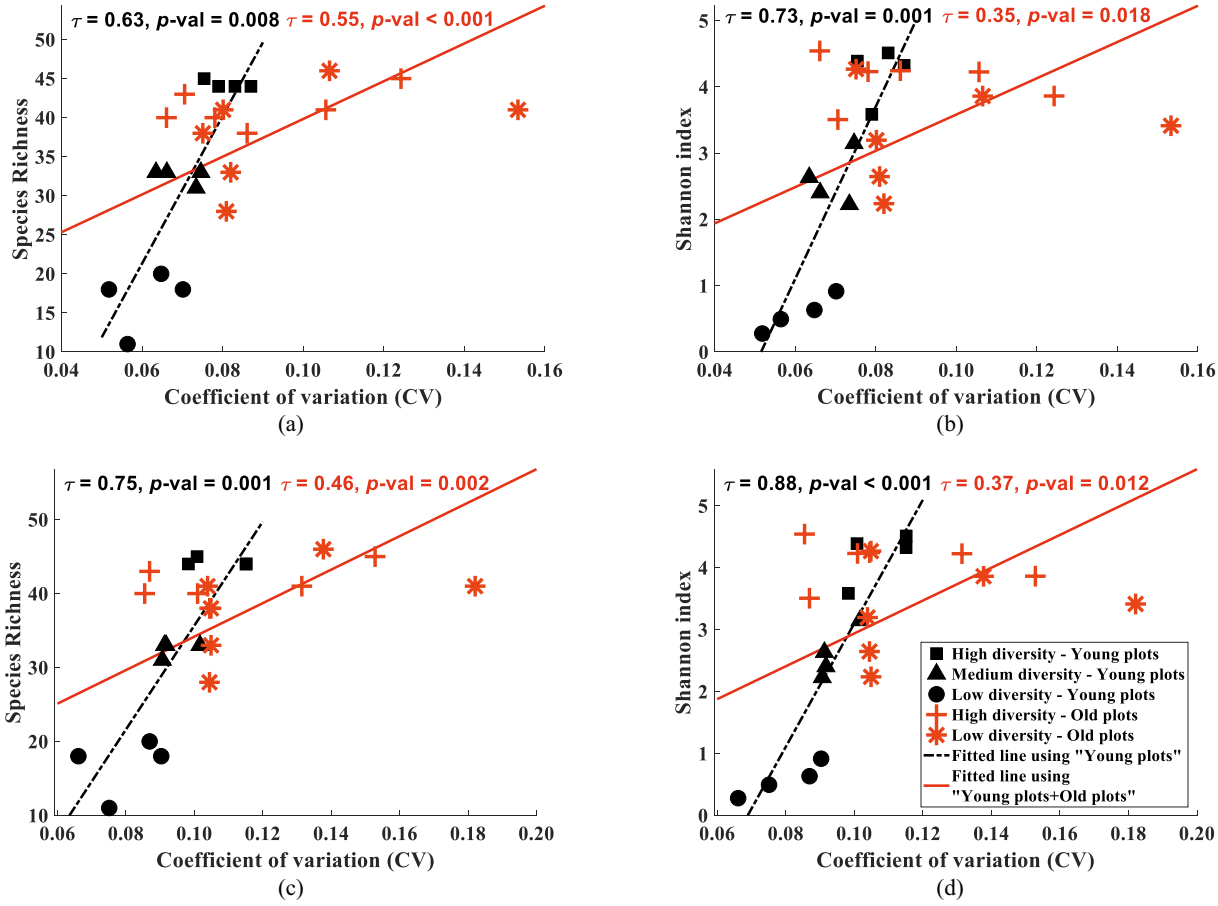

Fig. 2. Relationship between airborne spectral diversity (CV) and field-sampled α-diversity measured as species richness or Shannon index: a) species richness vs. CV at a spatial resolution of 1 m, b) Shannon index vs. CV at a spatial resolution of 1 m, (c) species richness vs. CV at a spatial resolution of 0.5 m, and (d) Shannon index vs. CV at a spatial resolution of 0.5 m. Black symbols represent young plots; red symbols represent old plots; the black dashed lines are fitted linear regressions for young plots, and the dark red solid lines are fitted lines to young and old plots combined. Spectral diversity-α-diversity relationships in the old plots (red symbols) are non-significant and fitted lines are not shown. (For interpretation of the references to color in this figure legend, the reader is referred to the web version of this article.)

In this equation, "·" represents the inner product, $\|\|_2$ is the *L*2-norm (a.k.a. Euclidean distance), $\overline{R}_L$ is the mean reflectance of the L^{th} plot, and $R_{K,\,L}$ is the reflectance of the K^{th} pixel (or observation) in the L^{th} plot. The length of both $\overline{R}_L$ and $R_{K,\,L}$ vectors is equal to the number of bands (all spectral bands were used in the spectral angle calculation). The output of this metric for every two input vectors is a scalar spectral angle between two vectors. If the reflectance of a pixel in a plot is similar to the mean reflectance of that plot, then the spectral angle values for that pixel will be small. The more different the vectors are, the larger the angle is. We calculated spectral angles for all pixels within a plot to depict spatial patterns of diversity. Another reason for using SAM to map spatial variation within each plot is its simplicity and independence from illumination variations (SAM uses the angles between reflectance vectors rather than length of the vectors).

2.5. Statistical analysis

The small sample size of the data set did not warrant using goodness of fit measures such as R^2 or Pearson correlation (Cramer, 1987). Instead, we used Kendall's rank correlation (τ) to assess the spectral diversity-α-diversity relationship (Kendall, 1938), a non-parametric measure of correlation, which is less sensitive to small sample sizes. To compare the correlations between spectral diversity and α-diversity under different conditions (spatial resolution and flight direction), instead of parametric solutions such as analysis of covariance (ANCOVA), we applied a permutation-based test (Legendre and Legendre, 1998) of the significance of difference in Kendall's τ coefficients with 10,000 permutations.

3. Results

3.1. Relationship between spectral diversity and α-diversity in the young plots

In our first analysis, we compared spectral diversity (CV calculated at the 60 m plot scale, Fig. 1a) to α-diversity (species richness and Shannon index calculated from field transects, Fig. 1b) using two different flight altitudes and pixel sizes. At 1 m spatial resolution, CV showed a strong relationship with species richness in the young plots (Kendall's τ coefficient of 0.63; Fig. 2a). When the abundance of species was considered using Shannon index, the relationship between α-diversity and CV improved (Kendall's τ coefficient of 0.73; Fig. 2b). At 0.5 m spatial resolution, CV was strongly associated with species richness in the young plots (Kendall's τ coefficient of 0.75; Fig. 2c). Similar to the coarser resolution image, when the evenness of the species was considered using Shannon index, CV showed a stronger relationship with α-diversity (Kendall's τ coefficient of 0.88; Fig. 2d). Similar to the West-East flights, in the North-South flights, spectral diversity showed strong relationships with α-diversity, and this relationship was stronger when α-diversity was expressed as Shannon index. Detailed results from the significant relationships (i.e. results from the young plots) are summarized in Table 3 (summary statistics expressed as R^2 are also provided in Table A4 in Appendix 1).

Table 3
Summary statistics expressed as the Kendall's τ coefficient for the "spectral diversity-species richness" and "spectral diversity-Shannon index" relationships for West-East and North-South flights at two spatial resolutions in the young plots. Summary statistics expressed as R^2 are also provided in Table A4 in Appendix 1.

Spectral diversity	Flight direction	Spatial resolution (m)	n	Species richness		Shannon index	
				Kendall's τ	*p*-Val	Kendall's τ	*p*-Val
CV	W-E	0.5	12	0.75	0.001	0.88	< 0.001
	N-S		12	0.66	0.005	0.70	0.002
	W-E	1	12	0.63	0.008	0.73	0.001
	N-S		12	0.72	0.002	0.73	0.001

Table 4
Permutation-based test (for N = 10,000 permutations) of the significance of difference in Kendall's τ coefficients at two spatial resolutions in the young plots. In this table, both the "spectral diversity-species richness" and "spectral diversity-Shannon index" relationships are presented.

Spectral diversity	Flight direction	Spatial resolution (m)	Species richness	Shannon index
			Difference in Kendall's τ	Difference in Kendall's τ
CV	W-E	0.5 1	Non-significant (*p*-val = 0.57)	Non-significant (*p*-val = 0.54)
	N-S	0.5 1	Non-significant (*p*-val = 0.81)	Non-significant (*p*-val = 0.95)

3.2. Impact of spatial scale and flight direction on spectral diversity-α-diversity relationship in the young plots

3.2.1. Spatial scale

While Kendall's τ coefficient of the spectral diversity-α-diversity relationship in the West-East flights improved when using the data with finer spatial resolution, the performance of spectral diversity metric in the North-South flights slightly weakened at finer spatial resolutions for both measures of α-diversity (i.e. species richness and Shannon index; Table 3). However, for both flight directions, the permutation-based test of significance showed that the difference between the spectral diversity-α-diversity relationship at two spatial resolutions was non-significant (the *p*-values of the test are presented in Table 4).

While there was no significant difference between the spectral diversity-α-diversity relationships obtained from the data with native resolutions (0.5 m and 1 m), our coarsened data set revealed a clear scale-dependence of this relationship (Fig. 3). When using species richness, the relationship became non-significant at pixel sizes of 5 m. As expected, the relationship between spectral diversity and Shannon index was stronger than that of the spectral diversity and species richness across scales. The relationship between spectral diversity and Shannon index became non-significant for pixels sizes of 6 m.

3.2.2. Flight direction

The results demonstrated that the influence of flight direction on the spectral diversity metric was small (Figs. 4–5). Although the Kendall's τ coefficient values indicated that in general the spectral diversity metrics obtained from the West-East flights (almost parallel to the solar principal plane) performed slightly better than those obtained from the North-South flights (column "Kendall's τ" in Table 3), the difference in the spectral diversity-α-diversity relationship (i.e. difference in the Kendall's τ coefficient) between the two flight directions was non-significant (Table 5).

3.3. Relationship between spectral diversity and α-diversity in the old plots

Although the relationship between spectral diversity and α-diversity (species richness and Shannon index) was strong in the young plots, in the old plots, this relationship became non-significant (red symbols in Fig. 2). When the data from both old and young plots were considered, the spectral diversity-α-diversity relationship appeared to saturate at high values of spectral diversity (instead of showing a continuous linear relationship).

To investigate the cause of the seemingly poor results from the old plots, we examined certain key assumptions of the study design relating plot-based imagery to transect-based field sampling. Although wide ranges of plot-based spectral diversity values were observed in the old plots with four plots showing high values, the ranges of the transect-based α-diversity values (species richness and Shannon index) were narrow (see Fig. 2). Plot maps using the spectral angle mapper indicated that while young plots were relatively homogeneous, the old plots were visibly heterogeneous (Fig. 6). In addition, plots with the highest spectral diversity in Fig. 2 are those yielding the highest spatial variability (plot numbers 18, 21, 17, and 24 in Fig. 6). In such cases of high spatial heterogeneity, the relationship between spectral diversity and α-diversity can become confounded by the mismatches in sampling

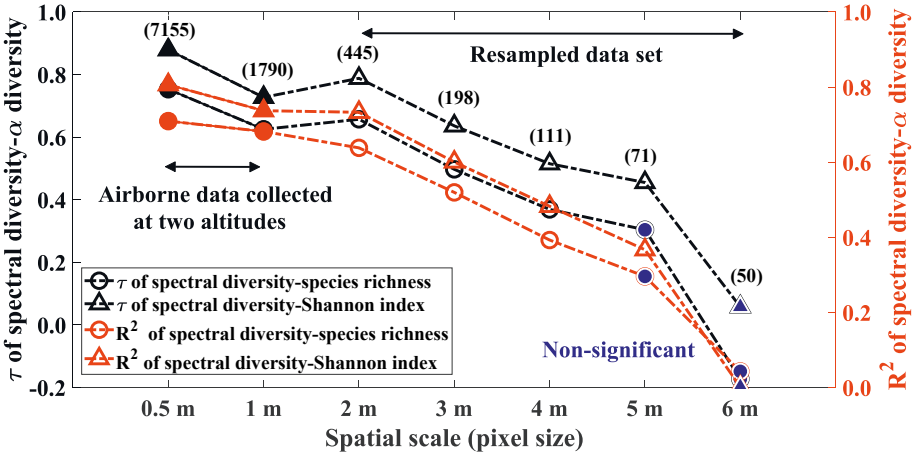

Fig. 3. Multiscale analysis of spectral diversity-α-diversity relationship in the young plots at different spatial resolutions expressed as the Kendall's τ coefficient (black lines and symbols) and proportion of explained variance (R^2, red lines and symbols). In this figure, solid points represent measured airborne data, and hollowed points represent resampled airborne data. Blue points indicate non-significant relationships. The numbers inside parentheses are the number of pixels within each plot at each resolution. (For interpretation of the references to color in this figure legend, the reader is referred to the web version of this article.)

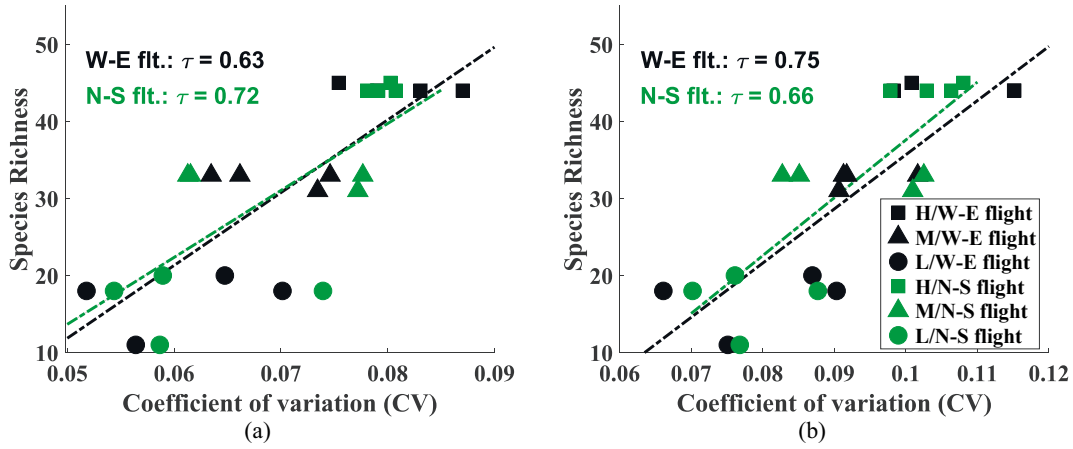

Fig. 4. Relationship between spectral diversity and species richness in the young plots using airborne data collected at two altitudes and two flight directions (four flights in total). (a) CV applied to airborne data with spatial resolution of 1 m, and (b) CV applied to airborne data with spatial resolution of 0.5 m. In these figures, black symbols and lines represent the West-East flights, and dark green symbols and lines represent the North-South flights. H, M, and L indicate plots with high, medium, and low planted diversity, respectively. (For interpretation of the references to color in this figure legend, the reader is referred to the web version of this article.)

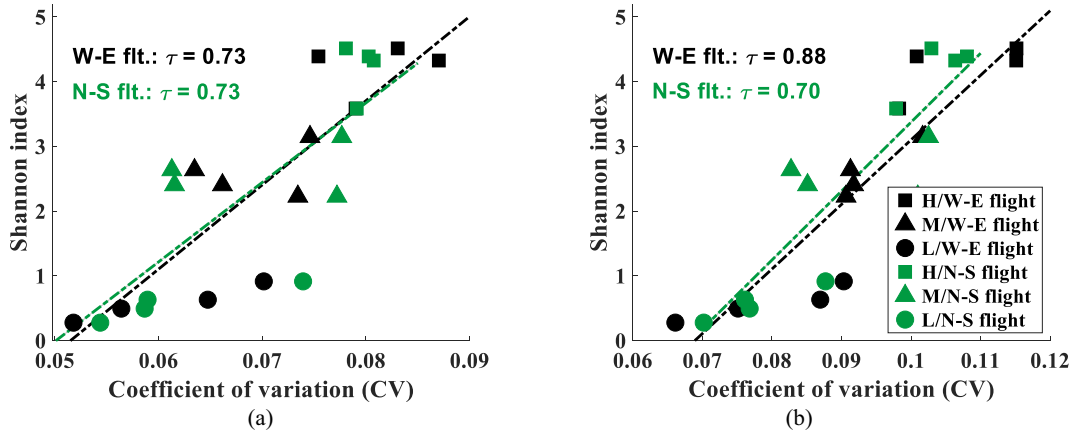

Fig. 5. Relationship between spectral diversity and Shannon index in the young plots using airborne data collected at two altitudes and two flight directions (four flights in total). (a) CV applied to airborne data with spatial resolution of 1 m, and (b) CV applied to airborne data with spatial resolution of 0.5 m. In this figure, black symbols and lines represent the West-East flights, and dark green symbols and lines represent the North-South flights. H, M, and L indicate plots with high, medium, and low planted diversity, respectively. (For interpretation of the references to color in this figure legend, the reader is referred to the web version of this article.)

geometry between plots and transects. To explore this possibility, we conducted a transect-based analysis of spectral diversity-α-diversity relationship (Fig. 7) where only the airborne pixels matching the approximate location of ground transects were sampled (and ignoring the pixels from the rest of the plot). This transect-based analysis made the spectral diversity values of the old plots become more aligned with those of the young plots (Fig. 7). One plot (#18) still displayed a high spectral diversity value in the transect-based analysis and did not align with the other points. Plot 18, which also had the highest variability in spectral angles among all plots (see Fig. 6), was detected as an outlier based on the median absolute deviation test and excluded from further transect-based analysis. The spectral diversity-α-diversity relationship in the old plots by themselves was still non-significant, presumably due to the small range of diversity values for these plots. However, the improved alignment attained in this analysis suggested that the mismatch between the field and airborne sampling can partly explain the different results originally obtained between young and old plots (Fig. 2).

Table 5
Permutation-based test of the significance of difference in Kendall's τ coefficients (for N = 10,000 permutations) at two flight directions in the young plots. In this table, both the "spectral diversity-species richness" and "spectral diversity-Shannon index" relationships are presented.

Spectral diversity	Flight direction	Spatial resolution (m)	Species richness	Shannon Index
			Difference in Kendall's τ	Difference in Kendall's τ
CV	W-E N-S	0.5	Non-significant (*p*-val = 0.47)	Non-significant (*p*-val = 0.27)
	W-E N-S	1	Non-significant (*p*-val = 0.56)	Non-significant (*p*-val = 0.93)

4. Discussion

Altogether, the results obtained from the airborne data at two altitudes and two flight directions showed 1) strong spectral diversity-α-diversity relationship in the young plots, 2) an improved relationship when the abundance-based metric (i.e. Shannon index) was used to express α-diversity, confirming the findings of others (Oldeland et al., 2010), 3) non-significant spectral diversity-α-diversity relationship in

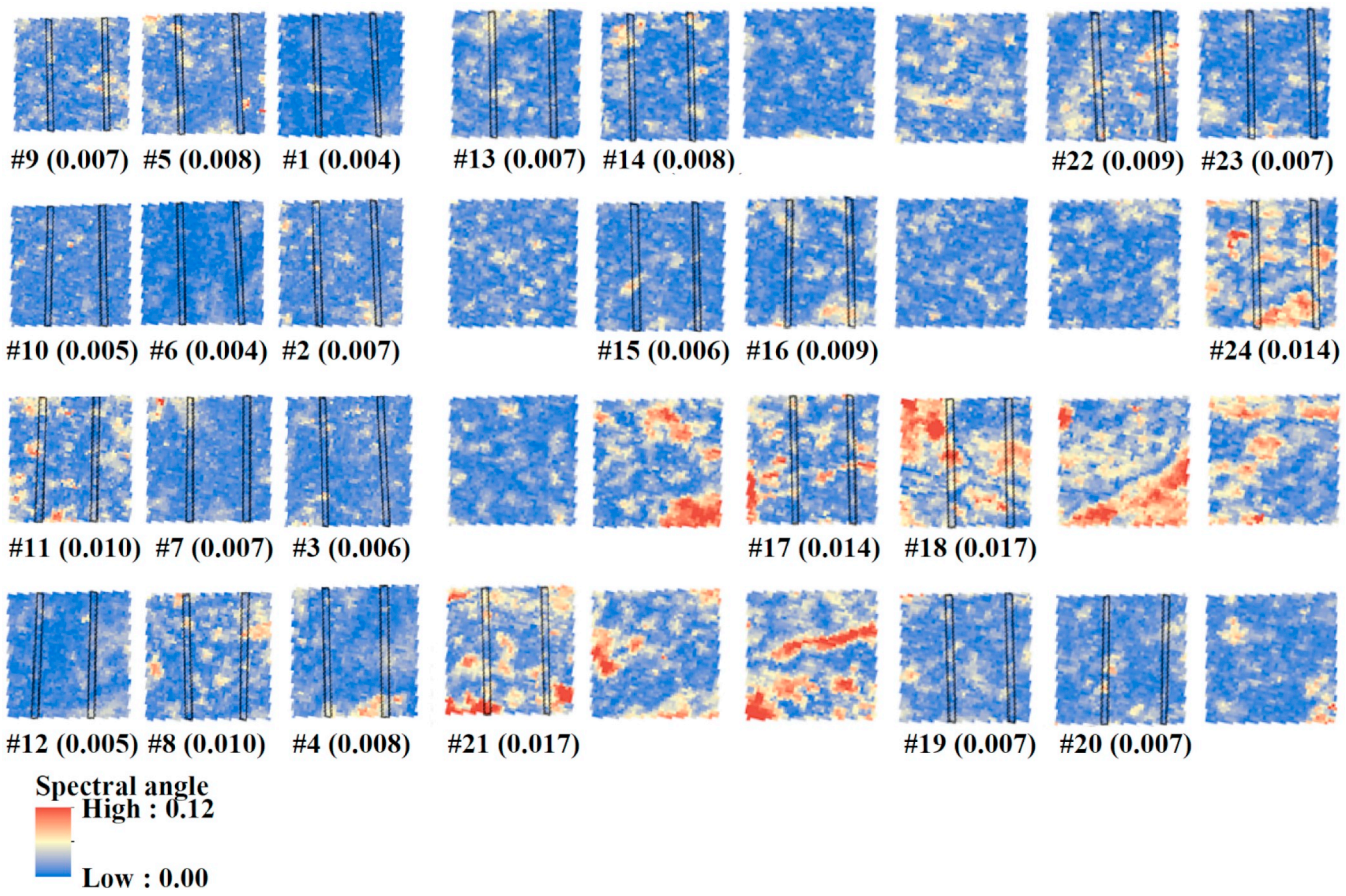

Fig. 6. Maps illustrating spatial heterogeneity within each plot using spectral angle mapper applied to the 1 m resolution data captured at the West-East flight direction. The approximate locations of species inventory transects (field sampling) are overlaid on the maps. These 2-meter wide transects are approximately 20 m and 40 m from the western edge of each plot. The numbers below the plots show the plot numbering scheme, and the numbers within parentheses show the standard deviation of spectral angles within each plot. To clearly show the patterns of spectral diversity, we applied histogram equalization to this map. The 0.5 m resolution map showed similar spatial patterns; therefore, only the 1 m resolution map is displayed here.

the old plots, 4) non-significant scale dependence of spectral diversity at 0.5 m and 1 m resolutions, but strong scale dependence in the coarsened data set over a wider range of spatial resolutions, and 5) slight impact of flight direction on the performance of spectral diversity metric.

4.1. Impact of spatial scale and flight direction on spectral diversity-α-diversity relationship

The scale-dependence of the spectral diversity-α-diversity relationship obtained from the airborne and coarsened data sets can guide future efforts to select appropriate pixel sizes in the design of airborne and spaceborne hyperspectral sensors for mapping biodiversity. Results of this study indicate that the spatial resolution provided by forthcoming satellite sensors (typically tens of meters) might be too coarse for capturing α-diversity in grasslands where each pixel can contain several species. To further investigate this, we would need to repeat similar studies to generate pixels with sizes comparable to those of spaceborne sensors, which would require collecting species inventories from much larger regions.

Another finding of this study was that the influence of flight direction (and hence sampling geometry) on the spectral diversity-α-diversity relationship was small (Figs. 4–5 and Table 5). The non-Lambertian property of vegetation surfaces has often been attributed to the structural properties of the canopy (Calleja et al., 2016), and can become quite striking for vegetation stands having clearly visible vertical structure (e.g. in the case of conifers or row crops). However, in our grassland plots, there was no significant bare soil exposure, neither were there a discernible row structure (a phenomenon common in croplands), presumably reducing the influence of canopy structure and flight direction on the measured signals. These observations may help explain why there were no significant differences in the results obtained from two different flight directions. However, it should be noted that modelling the impact of sun-target-sensor geometry on spectral reflectance is complicated and depends on issues such as viewing angle (nadir or off-nadir), solar angles, stage of development, canopy density, and subsequent soil exposure (Camacho de Coca et al., 2001; Kimes et al., 1980; Ranson et al., 1985). Our results were based on images acquired under similar solar angles and from identical grassland plots, and we suggest repeating similar experiments under different conditions (e.g. different vegetation types, different viewing and solar angles, and different seasons). However, the relatively small influence of flight direction suggests that sampling geometry may not be a major constraint for operational remote sensing of biodiversity in grassland ecosystems.

4.2. Spectral diversity-α-diversity in invaded plots

The shift in species composition and diversity over time in the old plots resulted from a combination of species spreading between plots and invasion by exotic weeds not intended to be part of the study design, both of which tended to even out the species richness differences across plots. To the degree that we are observing ecological succession – the replacement of one community type by another – our original study

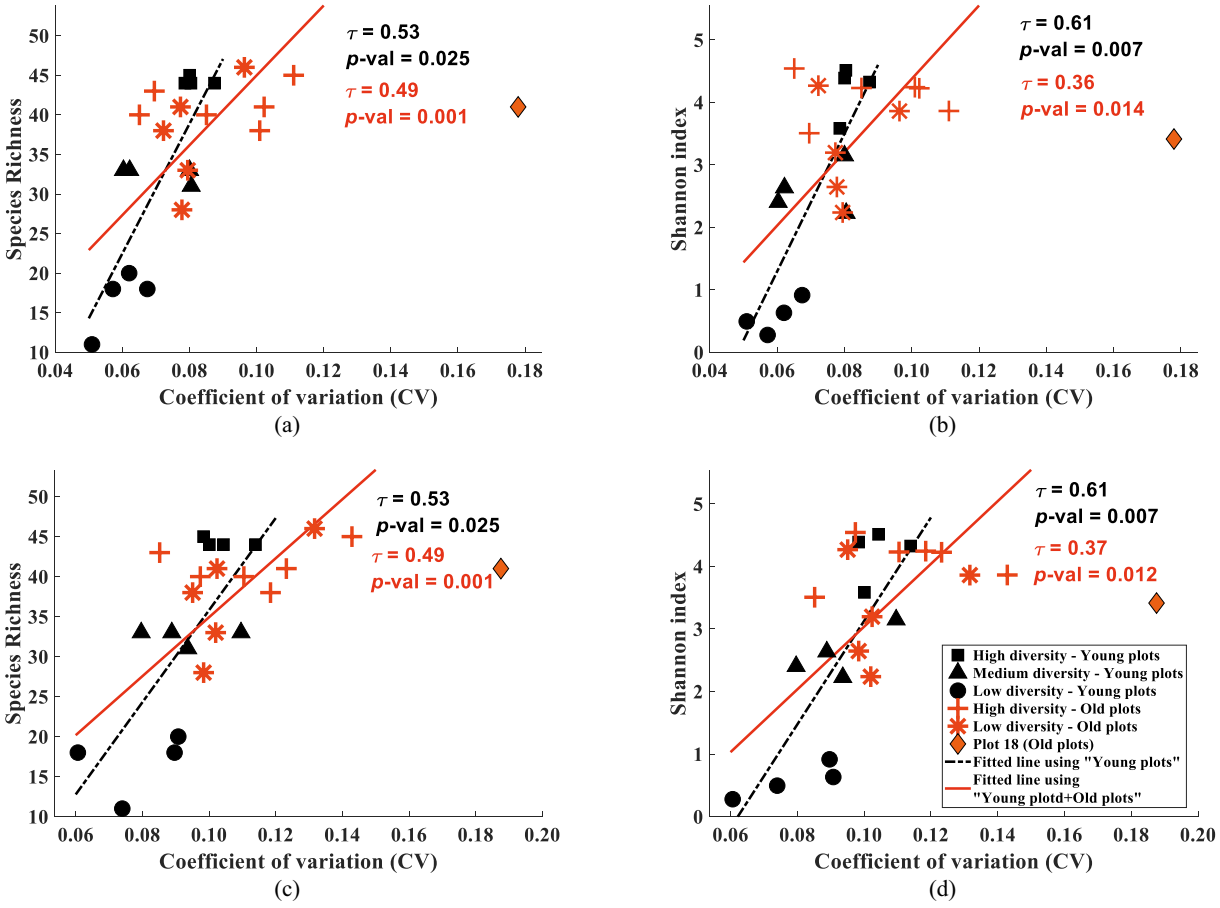

Fig. 7. The relationship between airborne spectral diversity (CV) and field-sampled α-diversity, obtained from the two transects within each plot. a) Species richness vs. CV at a spatial resolution of 1 m, b) Shannon index vs. CV at a spatial resolution of 1 m, (c) species richness vs. CV at a spatial resolution of 0.5 m, and (d) Shannon index vs. CV at a spatial resolution of 0.5 m. Black symbols represent young plots; red symbols represent old plots; the dark red diamond symbol shows plot 18, which was excluded from the analysis; the black dashed lines are fitted linear regressions to young plots, and the dark red solid lines are fitted lines to young and old plots combined. Spectral diversity-α-diversity relationships in the old plots (red symbols) are non-significant, and a fitted line is not given. (For interpretation of the references to color in this figure legend, the reader is referred to the web version of this article.)

goal of sampling α-diversity may have become undermined. Instead, in the old plots undergoing succession (invasion by exotic weeds), the metrics designed for α-diversity may have been confounded to some degree by β-diversity, reflecting a mismatch between idealized ecological concepts of diversity and actual dynamics of diversity observed across scales.

In addition, the difference in the spectral diversity-α-diversity relationships obtained from plot-based (Fig. 2) and transect-based (Fig. 7) analyses indicates a mismatch between our remote sensing analysis (based on pixels within a plot) and our field sampling (based on transects). A common limitation of species inventories is that they are typically collected from limited number of sampling points; therefore, not all taxa present in the community are measured. This undersampling (incompleteness or non-representativeness of species inventories) in field surveys introduces a potential error in measures of species diversity (e.g. species richness or Shannon index) (Beck et al., 2013; Beck and Schwanghart, 2010; Chao and Shen, 2003).

The old plots (but not the young plots) contained poison hemlock (*Conium maculatum*), which grew in large patches, and was visibly dry and non-photosynthetic at the time of data collection (showing early senescence, determined by browning of the foliage). The four old plots with the highest spectral diversity values (plot numbers 18, 21, 17, and 24) also contained sweet clover (*Melilotus officinalis*), which was taller than other species and found abundantly in the old plots (see Fig. A3 in Appendix for the contribution of different species to spectral diversity values). These phenological and structural features surely affected spectral properties of these invasive species and most likely contributed to spectral heterogeneity (shown in Fig. 6) in the old plots during the time of our overpass.

4.3. Remote sensing of biodiversity and design of the experimental plots

In this study, we were able to remotely detect biodiversity in a grassland experiment with different levels of diversity and large plots as part of a prairie restoration project. Comparable airborne data (e.g. spatial resolution of 0.75 m at the Cedar Creek Ecosystem Science Reserve's BioDIV experiment in Central Minnesota) showed much weaker spectral diversity-α-diversity relationships (Gholizadeh et al., 2018; Wang et al., 2018). On the other hand, a significant spectral diversity-species richness relationship ($R^2 = 0.34$) has been found using comparable airborne data (spatial resolution of 1.1 m) in a natural prairie grassland in southern Alberta, Canada (Wang et al., 2016). These notable differences between studies suggest several possible factors affecting the strength of the spectral diversity-biodiversity relationship for prairies including the spatial resolution of the data (as was discussed in Section 4.1), role of invasion (as was discussed in Section 4.2), degree of manipulation through management regimes (e.g. weeding or other disturbances), and plot design including the size of the plot (or uniform landscape patch) and number of species within the plots.

Frequent manipulation in biodiversity experiments (e.g. weeding as was the case at the Cedar Creek's BioDIV experiment) can lead to

challenges in remote sensing of biodiversity. With heavy manipulation, measures of spectral diversity can become more sensitive to factors such as productivity and plant cover (density) rather than biodiversity per se. Degree of soil exposure (which can be influenced by weeding) also influences the observed remote sensing reflectance such that spectral diversity does not reliably represent species diversity (Gholizadeh et al., 2018) because it is affected by the high spectral variation between green plants and soil. In the Wood River experiment, despite minor weed removal, all plots (low and high diversity) had comparable seeding density, and no significant soil cover was observed within the plots, providing a more favorable and possibly more realistic test of the effect of α-diversity on spectral diversity.

Plot size is another significant factor in remote sensing of biodiversity, especially in experimental plots, many of which involve small plots that do not match the scale of remote sensing observations. The declining spectral diversity-α-diversity relationship at coarser spatial resolutions in our multiscale analysis (Fig. 3) can be partly attributed to the sample size (number of pixels), where the sample size is limited by the size of our plots. When the plot size is large enough to easily exceed the scale (pixel size) of remote sensing observations, more spectral observations (i.e. pixels) are available (larger sample size) and therefore more reliable estimates of α-diversity can presumably be obtained. Increasing the plot area, also increases the number of species, via the species-area relationship (Preston, 1960), leading to a larger range of spectral diversity (spectral diversity-area relationship; Dahlin, 2016).

In addition to plot size, the species composition within plots is also important and ideally should represent naturally assembled grasslands. Plots at the Wood River site are approximately 60 × 60 m with species richness between 11 and 46 [35.33 ± 9.92; mean ± standard deviation]. The seed mixes in this site were collected within 100-mile radius of the restoration site, representing the species in the nearby prairies (Steinauer et al., 2003). Clearly, developing operational remote sensing methods for assessing biodiversity benefits from such experiments that closely resemble naturally assembled grasslands.

It is likely that differences in experimental design can influence the spectral diversity-α-diversity relationship. To achieve operational biodiversity monitoring systems based on remote sensing, we suggest establishing well-designed experiments from a remote sensing perspective. Such experiments should be designed to more closely resemble natural landscapes by minimizing human-caused manipulations, consider the mismatch between the remote sensing sampling and ground sampling, and have widely varying levels of species diversity.

4.4. Future work

The sensor used in this study had fine spectral resolution but covered only the visible and near-infrared (VNIR) region from ~400 nm to 1000 nm. However, some of the current and forthcoming airborne hyperspectral sensors such as AVIRIS (Green et al., 1998), HYMAP (Cocks et al., 1998), AVIRIS-NG (Hamlin et al., 2011), and AisaDUAL (Specim Ltd) operate over broader wavelength ranges from 400 nm to 2500 nm with spectral sampling between ~5 nm–20 nm. In principle, full-range imagers are sensitive to additional vegetation traits (Serbin et al., 2014; Ustin et al., 2004), which have been shown to affect spectral diversity measured via remote sensing (Asner and Martin, 2009; Carlson et al., 2007). Therefore, although the VNIR sensors are more accessible due to their low cost and smaller payload, using full range imaging sensors to examine the impact of broader ranges of biochemical and structural traits may be warranted.

Our experiment at Wood River contained both warm-season and cool-season grasses. However, natural grasslands of North America can have different species composition with different phenology. While warm-season (C_4) grasses dominate some of the North American prairies, cool-season (C_3) species or a mixture of both can dominate others (Anderson, 2006; Samson and Knopf, 1994; Wang et al., 2013). Further studies should test how well our study findings can be generalized to other prairie types (e.g. tallgrass, shortgrass, and mixed-grass) with different functional group composition (C_3 and C_4 species). In addition, although studies like this are expanding our knowledge of remotely detecting prairie diversity, further studies of other short-statured vegetation (e.g. shrublands and tundra) are also needed to develop suitable methods for routine operational assessment of spectral diversity.

Reflectance data are an amalgamation of biochemical properties of vegetation and vegetation structure, all of which change over time (Asner and Martin, 2009; Chavana-Bryant et al., 2017; Ustin et al., 2009). We did not quantify the variation of each component over time, nor did we estimate the scale dependence of each component individually. Therefore, further experiments at this and other sites examining the changes in spectral diversity-α-diversity relationship over the growing season at different spatial scales remain necessary if we are to develop robust, operational remote sensing methods of assessing biodiversity.

5. Conclusions

We examined the relationship between spectral diversity (expressed as coefficient of variation) and α-diversity (expressed as species richness and Shannon index) in a large-scale prairie restoration experiment in Wood River, Central Nebraska, USA. A strong spectral diversity-α-diversity relationship was evident for young plots where the original study design remained intact, and this relationship became stronger when species abundance was taken into account. However, the relationship was non-significant in the old plots, which had been affected by the spread of species between plots and invasion of exotic species. This non-significant relationship was partly attributable to the different spectral and structural properties of invasive species, the contrasting phenology of planted and invasive species, and the convergence of all plots towards similar levels of diversity. Differences in spectral diversity-α-diversity relationships at 0.5 m and 1 m resolutions were negligible, but results obtained from a coarsened data set simulating a wider range of spatial resolutions displayed a declining spectral diversity-α-diversity relationship at coarser spatial resolutions and non-significant relationships at pixel sizes above 4–5 m. This result suggested that direct assessment of plot-scale α-diversity via spectral diversity in grasslands, while clearly possible with airborne platforms, may not be possible with most satellite sensors. Results obtained from two flight directions were not significantly different, suggesting that sampling geometry had only minor influence on spectral diversity.

The observation that airborne spectral diversity can provide a good proxy for α-diversity in grasslands provides a strong foundation for the ongoing development of operational airborne methods for assessing biodiversity and demonstrate the value of an experimental remote sensing approach. We recommend more attention to sampling design that explicitly considers the relationship between field sampling and airborne sampling, the degree and nature of experimental manipulation, and temporal effects (phenology and succession). Future work should repeat experiments such as this at a range of natural and restored prairies across a wider range of seasons and conditions. Careful coupling to field sampling design and knowledge of plot successional stage remain important to proper interpretation of the results.

Acknowledgements

Many thanks to two anonymous reviewers and the associate editor for providing feedback and insightful comments on this manuscript. We acknowledge The Nature Conservancy, its staff, and all the people who helped us during our field campaign. We specifically thank Nelson Winkel (TNC) who provided valuable information about the study area at the early stages of this experiment and assisted us during field data collection. We express our sincere gratitude to Rick Perk (Center for Advanced Land Management Information Technologies at UNL) for collecting the airborne data. We thank Kim Helzer for providing the

plant diversity inventory, Bryan Leavitt (UNL) and Katherine Hogan (TNC) for their invaluable field assistance. We also express our gratitude to Dr. Zheng Xu (UNL) for his advice on statistical analysis. Special thanks to Dr. Craig Allen (UNL) for helping us to improve the design of our experiment. We also thank Donnette Thayer for assistance in preparing the spectral diversity maps. This work was supported by NSF/NASA Dimensions of Biodiversity Program grant DEB-1342823 to J.A.G. and A.I.Z., DEB-1342872 to J.C.B., and DEB-1342778 to P.A.T. Mention of trade names does not imply endorsement by the authors.

Author contributions

H.G. and J.A.G. designed and conceived the study. H.G., J.A.G., J.C.B., P.A.T, G.Y.H., R.Y., and R.M.M. contributed to the fieldwork. J.C.B. and A.K.S. designed the plant diversity sampling. J.C.B. managed the plant diversity sampling and calculated plant diversity from field data. H.G. analyzed the data. H.G., J.A.G., J.C.B., P.A.T., A.I.Z., and C.J.H. contributed to writing the manuscript. All authors read and approved the manuscript.

Appendix A. Supplementary data

Supplementary data to this article can be found online at https://doi.org/10.1016/j.rse.2018.10.037.

References

Anderson, R.C., 2006. Evolution and origin of the Central Grassland of North America: climate, fire, and mammalian grazers. J. Torrey Bot. Soc. 133, 626–647.
Asner, G.P., Martin, R.E., 2009. Airborne spectranomics: mapping canopy chemical and taxonomic diversity in tropical forests. Front. Ecol. Environ. 7, 269–276.
Asner, G.P., Knapp, D.E., Kennedy-Bowdoin, T., Jones, M.O., Martin, R.E., Boardman, J., Hughes, R.F., 2008. Invasive species detection in Hawaiian rainforests using airborne imaging spectroscopy and LiDAR. Remote Sens. Environ. 112, 1942–1955.
Baldi, G., Guerschman, J.P., Paruelo, J.M., 2006. Characterizing fragmentation in temperate South America grasslands. Agric. Ecosyst. Environ. 116, 197–208.
Beck, J., Schwanghart, W., 2010. Comparing measures of species diversity from incomplete inventories: an update. Methods Ecol. Evol. 1, 38–44.
Beck, J., Holloway, J.D., Schwanghart, W., 2013. Undersampling and the measurement of beta diversity. Methods Ecol. Evol. 4, 370–382.
Bevans, R.A., 2017. Plant Diversity Influences the Structure and Function of a Restored Prairie and its Responses to Added Disturbances. School of Natural Resources, Lincoln, Nebraska: University of Nebraska.
Buchanan, G.M., Nelson, A., Mayaux, P., Hartley, A., Donald, P.F., 2009. Delivering a global, terrestrial, biodiversity observation system through remote sensing. Conserv. Biol. 23, 499–502.
Calleja, J.F., Recondo, C., Peón, J., Fernández, S., de la Cruz, F., González-Piqueras, J., 2016. A new method for the estimation of broadband apparent albedo using hyperspectral airborne hemispherical directional reflectance factor values. Remote Sens. 8, 183.
Camacho de Coca, F., Gilabert, M., Meliá, J., 2001. Bidirectional reflectance factor analysis from field radiometry and HyMap data. In: The Final Results Workshop on DAISEX (Digital AIrborne Spectrometer EXperiment), pp. 163–175 (Noordwijk, The Netherlands).
Carlson, K.M., Asner, G.P., Hughes, R.F., Ostertag, R., Martin, R.E., 2007. Hyperspectral remote sensing of canopy biodiversity in Hawaiian lowland rainforests. Ecosystems 10, 536–549.
Carter, G.A., Knapp, A.K., Anderson, J.E., Hoch, G.A., Smith, M.D., 2005. Indicators of plant species richness in AVIRIS spectra of a mesic grassland. Remote Sens. Environ. 98, 304–316.
Cavender-Bares, J., Gamon, J.A., Hobbie, S.E., Madritch, M.D., Meireles, J.E., Schweiger, A.K., Townsend, P.A., 2017. Harnessing plant spectra to integrate the biodiversity sciences across biological and spatial scales. Am. J. Bot. 104, 966–969.
Chao, A., Shen, T.-J., 2003. Nonparametric estimation of Shannon's index of diversity when there are unseen species in sample. Environ. Ecol. Stat. 10, 429–443.
Chapin, F.S., Sala, O.E., Burke, I.C., Grime, J.P., Hooper, D.U., Lauenroth, W.K., Lombard, A., Mooney, H.A., Mosier, A.R., Naeem, S., Pacala, S.W., Roy, J., Steffen, W.L., Tilman, D., 1998. Ecosystem consequences of changing biodiversity. Bioscience 48, 45–52.
Chavana-Bryant, C., Malhi, Y., Wu, J., Asner, G.P., Anastasiou, A., Enquist, B.J., Caravasi, E.G.C., Doughty, C.E., Saleska, S.R., Martin, R.E., Gerard, F.F., 2017. Leaf aging of Amazonian canopy trees as revealed by spectral and physiochemical measurements. New Phytol. 214, 1049–1063.
Clark, C.M., Tilman, D., 2008. Loss of plant species after chronic low-level nitrogen deposition to prairie grasslands. Nature 451, 712.
Cocks, T., Jenssen, R., Stewart, A., Wilson, I., Shields, T., 1998. The HyMapTM airborne hyperspectral sensor: the system, calibration and performance. In: Proceedings of the 1st EARSeL Workshop on Imaging Spectroscopy. EARSeL, pp. 37–42.
Conel, J.E., Green, R.O., Vane, G., Bruegge, C.J., Alley, R.E., 1987. AIS-2 radiometry and a comparison of methods for the recovery of ground reflectance. In: Vane, G. (Ed.), Third Airborne Imaging Spectrometer Data Analysis Workshop. JPL Publication, Pasadena, CA, pp. 18–47.
Cramer, J.S., 1987. Mean and variance of R2 in small and moderate samples. J. Econ. 35, 253–266.
Dahlin, K.M., 2016. Spectral diversity area relationships for assessing biodiversity in a wildland–agriculture matrix. Ecol. Appl. 26, 2758–2768.
Darvishzadeh, R., Atzberger, C., Skidmore, A., Schlerf, M., 2011. Mapping grassland leaf area index with airborne hyperspectral imagery: a comparison study of statistical approaches and inversion of radiative transfer models. ISPRS J. Photogramm. Remote Sens. 66, 894–906.
Dell'Endice, F., 2008. Improving the performance of hyperspectral pushbroom imaging spectrometers for specific science applications. In: ISPRS 2008: Proceedings of the XXI Congress: Silk Road for Information from Imagery: The International Society for Photogrammetry and Remote Sensing, pp. 215–220 (Beijing, China).
Gaitán, J.J., Bran, D., Oliva, G., Ciari, G., Nakamatsu, V., Salomone, J., Ferrante, D., Buono, G., Massara, V., Humano, G., 2013. Evaluating the performance of multiple remote sensing indices to predict the spatial variability of ecosystem structure and functioning in Patagonian steppes. Ecol. Indic. 34, 181–191.
Gholizadeh, H., Gamon, J.A., Zygielbaum, A.I., Wang, R., Schweiger, A.K., Cavender-Bares, J., 2018. Remote sensing of biodiversity: soil correction and data dimension reduction methods improve assessment of α-diversity (species richness) in prairie ecosystems. Remote Sens. Environ. 206, 240–253.
Gillespie, T.W., Foody, G.M., Rocchini, D., Giorgi, A.P., Saatchi, S., 2008. Measuring and modelling biodiversity from space. Prog. Phys. Geogr. 32, 203–221.
Goodin, D.G., Gao, J., Henebry, G.M., 2004. The effect of solar illumination angle and sensor view angle on observed patterns of spatial structure in tallgrass prairie. IEEE Trans. Geosci. Remote Sens. 42, 154–165.
Gougeon, F.A., 1995. Comparison of possible multispectral classification schemes for tree crowns individually delineated on high spatial resolution MEIS images. Can. J. Remote. Sens. 21, 1–9.
Green, R.O., Eastwood, M.L., Sarture, C.M., Chrien, T.G., Aronsson, M., Chippendale, B.J., Faust, J.A., Pavri, B.E., Chovit, C.J., Solis, M., 1998. Imaging spectroscopy and the airborne visible/infrared imaging spectrometer (AVIRIS). Remote Sens. Environ. 65, 227–248.
Guanter, L., Kaufmann, H., Segl, K., Foerster, S., Rogass, C., Chabrillat, S., Kuester, T., Hollstein, A., Rossner, G., Chlebek, C., 2015. The EnMAP spaceborne imaging spectroscopy mission for earth observation. Remote Sens. 7, 8830–8857.
Guo, X., Wilmshurst, J., McCanny, S., Fargey, P., Richard, P., 2015. Measuring spatial and vertical heterogeneity of grasslands using remote sensing techniques. J. Environ. Inf. 3, 24–32.
Hamlin, L., Green, R., Mouroulis, P., Eastwood, M., Wilson, D., Dudik, M., Paine, C., 2011. Imaging spectrometer science measurements for terrestrial ecology: AVIRIS and new developments. In: Aerospace Conference, 2011 IEEE. IEEE, pp. 1–7.
Hooper, D.U., Adair, E.C., Cardinale, B.J., Byrnes, J.E., Hungate, B.A., Matulich, K.L., Gonzalez, A., Duffy, J.E., Gamfeldt, L., O'Connor, M.I., 2012. A global synthesis reveals biodiversity loss as a major driver of ecosystem change. Nature 486, 105–108.
Jetz, W., Cavender-Bares, J., Pavlick, R., Schimel, D., Davis, F.W., Asner, G.P., Guralnick, R., Kattge, J., Latimer, A.M., Moorcroft, P., Schaepman, M.E., Schildhauer, M.P., Schneider, F.D., Schrodt, F., Stahl, U., Ustin, S.L., 2016. Monitoring plant functional diversity from space. Nat. Plants 2, 193.
Kendall, M.G., 1938. A new measure of rank correlation. Biometrika 30, 81–93.
Kerr, J.T., Ostrovsky, M., 2003. From space to species: ecological applications for remote sensing. Trends Ecol. Evol. 18, 299–305.
Kimes, D.S., Smith, J.A., Ranson, K.J., 1980. Vegetation reflectance measurements as a flmction of solar zenith angle. Photogramm. Eng. Remote. Sens. 46, 1563–1573.
Kruse, F.A., Lefkoff, A., Boardman, J., Heidebrecht, K.B., Shapiro, A.T., Barloon, P.J., Goetz, A.F.H., 1993. The spectral image processing system (SIPS)—interactive visualization and analysis of imaging spectrometer data. Remote Sens. Environ. 44, 145–163.
Kustas, W., Norman, J., 1996. Use of remote sensing for evapotranspiration monitoring over land surfaces. Hydrol. Sci. J. 41, 495–516.
Lauver, C.L., 1997. Mapping species diversity patterns in the Kansas shortgrass region by integrating remote sensing and vegetation analysis. J. Veg. Sci. 8, 387–394.
Lee, C.M., Cable, M.L., Hook, S.J., Green, R.O., Ustin, S.L., Mandl, D.J., Middleton, E.M., 2015. An introduction to the NASA Hyperspectral InfraRed Imager (HyspIRI) mission and preparatory activities. Remote Sens. Environ. 167, 6–19.
Legendre, P., Legendre, L., 1998. Numerical Ecology. Elsevier Science, Amsterdam.
Naeem, S., Chazdon, R., Duffy, J.E., Prager, C., Worm, B., 2016. Biodiversity and human well-being: an essential link for sustainable development. Proc. R. Soc. B 283, 20162091.
Nagendra, H., 2001. Using remote sensing to assess biodiversity. Int. J. Remote Sens. 22, 2377–2400.
Nemec, K.T., Allen, C.R., Helzer, C.J., Wedin, D.A., 2013. Influence of richness and seeding density on invasion resistance in experimental tallgrass prairie restorations. Ecol. Restor. 31, 168–185.
Oldeland, J., Wesuls, D., Rocchini, D., Schmidt, M., Jürgens, N., 2010. Does using species abundance data improve estimates of species diversity from remotely sensed spectral heterogeneity? Ecol. Indic. 10, 390–396.
Oldeman, L., 1994. The global extent of soil degradation. In: Soil Resilience and Sustainable Land Use. 9.
Preston, F., 1960. Time and space and the variation of species. Ecology 41, 611–627.
Ramankutty, N., Evan, A.T., Monfreda, C., Foley, J.A., 2008. Farming the planet: 1. Geographic distribution of global agricultural lands in the year 2000. Glob.

Biogeochem. Cycles 22.
Ranson, K.J., Daughtry, C.S.T., L.B.L., Bauer, M.E., 1985. Sun-view angle effects on reflectance factors of corn canopies. Remote Sens. Environ. 18, 147–161.
Rocchini, D., Balkenhol, N., Carter, G.A., Foody, G.M., Gillespie, T.W., He, K.S., Kark, S., Levin, N., Lucas, K., Luoto, M., 2010. Remotely sensed spectral heterogeneity as a proxy of species diversity: recent advances and open challenges. Eco. Inform. 5, 318–329.
Samson, F., Knopf, F., 1994. Prairie conservation in North America. Bioscience 44, 418–421.
Schäfer, E., Heiskanen, J., Heikinheimo, V., Pellikka, P., 2016. Mapping tree species diversity of a tropical montane forest by unsupervised clustering of airborne imaging spectroscopy data. Ecol. Indic. 64, 49–58.
Schramm, P., 1990. Prairie restoration: a twenty-five year perspective on establishment and management. In: Smith, D.D., Jacob, C.A. (Eds.), Proceedings of the Twelfth North American Prairie Conference. University of Northern Iowa, Cedar Fall, Iowa, pp. 169–177.
Schweiger, A.K., Cavender-Bares, J., Townsend, P.A., Hobbie, S.E., Madritch, M.D., Wang, R., Tilman, D., Gamon, J.A., 2018. Plant spectral diversity integrates functional and phylogenetic components of biodiversity and predicts ecosystem function. Nat. Ecol. Evol. 2, 976–982.
Seaquist, J., Olsson, L., Ardö, J., 2003. A remote sensing-based primary production model for grassland biomes. Ecol. Model. 169, 131–155.
Serbin, S.P., Singh, A., McNeil, B.E., Kingdon, C.C., Townsend, P.A., 2014. Spectroscopic determination of leaf morphological and biochemical traits for northern temperate and boreal tree species. Ecol. Appl. 24, 1651–1669.
Shannon, C.E., 1948. A mathematical theory of communication. Bell Syst. Tech. J. 27, 379–423.
Shibayama, M., Wiegand, C., 1985. View azimuth and zenith, and solar angle effects on wheat canopy reflectance. Remote Sens. Environ. 18, 91–103.
Skidmore, A.K., Pettorelli, N., Coops, N.C., Geller, G.N., Hansen, M., Lucas, R., Mücher, C.A., O'Connor, B., Paganini, M., Pereira, H.M., Schaepman, M.E., Turner, W., Wang, T., Wegmann, M., 2015. Agree on biodiversity metrics to track from space: ecologists and space agencies must forge a global monitoring strategy. Nature 523, 403–405.
Steinauer, G., Whitney, B., Adams, K., Bullerman, M., Helzer, C., 2003. A Guide to Prairie and Wetland Restoration in Eastern Nebraska. Prairie Plains Resource Institute and the Nebraska Game and Parks Commission, Aurora.
Suding, K.N., 2011. Toward an era of restoration in ecology: successes, failures, and opportunities ahead. Annu. Rev. Ecol. Evol. Syst. 42.
Tilman, D., Reich, P.B., Isbell, F., 2012. Biodiversity impacts ecosystem productivity as much as resources, disturbance, or herbivory. Proc. Natl. Acad. Sci. 109, 10394–10397.
Tovar, C., Seijmonsbergen, A.C., Duivenvoorden, J.F., 2013. Monitoring land use and land cover change in mountain regions: an example in the Jalca grasslands of the Peruvian Andes. Landsc. Urban Plan. 112, 40–49.
Turner, W., 2014. Sensing biodiversity. Science 346, 301–302.
Turner, W., Spector, S., Gardiner, N., Fladeland, M., Sterling, E., Steininger, M., 2003. Remote sensing for biodiversity science and conservation. Trends Ecol. Evol. 18, 306–314.
Ustin, S.L., Gamon, J.A., 2010. Remote sensing of plant functional types. New Phytol. 186, 795–816.
Ustin, S.L., Roberts, D.A., Gamon, J.A., Asner, G.P., Green, R.O., 2004. Using imaging spectroscopy to study ecosystem processes and properties. AIBS Bull. 54, 523–534.
Ustin, S.L., Gitelson, A.A., Jacquemoud, S., Schaepman, M., Asner, G.P., Gamon, J.A., Zarco-Tejada, P., 2009. Retrieval of foliar information about plant pigment systems from high resolution spectroscopy. Remote Sens. Environ. 113, S67–S77.
Villnäs, A., Norkko, J., Hietanen, S., Josefson, A.B., Lukkari, K., Norkko, A., 2013. The role of recurrent disturbances for ecosystem multifunctionality. Ecology 94, 2275–2287.
Waide, R., Willig, M., Steiner, C., Mittelbach, G., Gough, L., Dodson, S., Juday, G., Parmenter, R., 1999. The relationship between productivity and species richness. Annu. Rev. Ecol. Syst. 30, 257–300.
Wall, D.H., Nielsen, U.N., Six, J., 2015. Soil biodiversity and human health. Nature 528, 69.
Wang, C., Jamison, B.E., Spicci, A.A., 2010. Trajectory-based warm season grassland mapping in Missouri prairies with multi-temporal ASTER imagery. Remote Sens. Environ. 114, 531–539.
Wang, C., Hunt Jr., E.R., Zhang, L., Guo, H., 2013. Phenology-assisted classification of C3 and C4 grasses in the US Great Plains and their climate dependency with MODIS time series. Remote Sens. Environ. 138, 90–101.
Wang, R., Gamon, J.A., Emmerton, C.A., Li, H., Nestola, E., Pastorello, G.Z., Menzer, O., 2016. Integrated analysis of productivity and biodiversity in a southern Alberta prairie. Remote Sens. 8, 214.
Wang, R., Gamon, J.A., Cavender-Bares, J., Townsend, P.A., Zygielbaum, A.I., 2018. The spatial sensitivity of the spectral diversity-biodiversity relationship: an experimental test in a prairie grassland. Ecol. Appl. 28, 541–556.
Weaver, J.E., 1954. North American Prairie. Johnson Publishing Co, Lincoln, NE.